Int. J. Nanosci. Nanotechnol., Vol. 12, No. 3, Sept. 2016, pp. 167-174

Preparation of Polyaniline-Polystyrene-ZnO Nanocomposite and Characterization of Its Anti-Corrosive Performance

Reza Layeghi[1, 2], Maryam Farbodi[1, 2,*] and Niloufar Ghalebsaz-Jeddi[2]

[1]Department of Chemistry, East Azarbayjan Science and Research Branch, Islamic Azad University, Tabriz, Iran

[2]Department of Chemistry, Tabriz Branch, Islamic Azad University, Tabriz, Iran

(*) Corresponding author: m.farbodi@iaut.ac.ir
(Received: 28 May 2015 and Accepted: 17 June 2016)

Abstract

In this research, firstly polyaniline-zinc oxide (PANI-ZnO) nanocomposite was successfully synthesized by chemical polymerization of aniline in the presence of ZnO nanoparticles and then, 5%, 10% and 15% solutions of PANI–ZnO nanocomposites were mixed with a solution of polystyrene (PS) in tetrahydrofurane (THF) and PANI-PS-ZnO nanocomposites were obtained. The prepared nanocomposites were used as coating on iron coupons by solution casting method and their anti corrosive performance were studied by open circuit potential (OCP) and Tafel techniques in 3.5% NaCl solution as corrosive environment. The obtained results showed that the coating of PS-[PANI-ZnO 10%] nanocomposite had superior corrosion protection effect on iron sample compared to that of pure PANI, PANI–ZnO nanocomposite, PANI-PS composite and two other PANI-PS-ZnO nanocomposite coatings. Cyclic voltammetry (CV) studies showed that the prepared PS-[PANI-ZnO 10%] nanocomposite was electroactive and this property was reversible and stable. Fourier transform infrared (FTIR) spectroscopy and scanning electron microscopy (SEM) techniques were used to characterize the composition and structure of PS-[PANI-ZnO 10%] nanocomposite. To study thermal stability of PS-[PANI-ZnO 10%] nanocomposite, thermogravimetric analysis (TGA) was used.

Keywords: *Corrosion, Nanocomposite, Polyaniline, Polystyrene, ZnO nanoparticle.*

1. INRODUCTION

Intrinsically conducting polymers (ICPs) have received considerable attention due to their similar electrical and optical properties as metals and mechanical properties and processability as polymers [1]. ICPs are used in many applications such as batteries [2], sensors [3], removal of toxic ions from water [4], antistatic coatings [5], broadband EMI (Electromagnetic_shielding) shielding [6], and anticorrosive coatings [7-9]. The undesired corrosion phenomenon is a potential problem in the world of industries that influences the economy of countries. Electrochemically active ICPs protect metals by acting as barrier layer between the metal and corrosive environment and also they are among anodic inhibitors by exhibiting some kinds of anodic protections on metals [10].

Although, a variety of ICPs have been studied as corrosion protection coatings [11,12], but polyaniline (PANI) has been the most often researched due to its high conductivity properties, environment stability, low cost and straightforward synthesis [7-10]. On the other hand, the applications of PANI are limited by its poor processability and week mechanical properties. Preparing of PANI composite with other conventional polymers is one of the most studied ways to improve processability and mechanical properties of PANI [1]. A variety of studies have been reported on the preparing of PANI composite with processiable polymers such

as polystyrene [1] and PVC (polyvinyl chloride) [13].

With the appearance of nanotechnology, nanofillers play significant roles in the improvement of mechanical, thermal, electrical and anticorrosive properties of polymers [14-20]. For example, one of the most effective and powerful anticorrosive coatings is zinc (Zn)–polymer system. Recently PANI-Zn composites and nanocomposites have been prepared and applied as anticorrosive coatings on iron. According to the results, PANI-Zn nanocomposite coatings and films have better corrosion protection effect compared to the PANI-Zn composite films [10].

Studies have shown that PANI forms a passive oxide layer on the iron surface. This oxide layer is mainly of a Fe_2O_3 layer. The protection mechanism of iron by doped PANI is shown that PANI redox couple (Emeraldine salt and Leuco base) has been regarded as being responsible for establishing the potential of iron in the passive region. The Leuco base that has been formed is cyclically oxidized to Emeraldine salt again by the reduction of oxygen so that the potential of iron is always maintained in the passive region [21].

In addition, it has been shown that, using zinc oxide (ZnO) nanoparticles to prepare PANI nanocomposite caused to improve anticorrosive properties of PANI [7]. ZnO is a semiconductor with a 3.37 eV band-gap and is used in many fields due to low cost, high stability and high ultraviolet absorption. Olad and et.al prepared PVC/PANI-ZnO nanocomposie and studied its anticorrosive properties on the iron. According to the results, PVC/PANI-ZnO nanocomposite showed dramatically increased corrosion protection effect compared to that of uncoated iron and pure PANI anticorrosive coatings. In addition, they showed that the use of a conventional polymer can improve the barrier and mechanical properties of PANI [7].

In this work, PANI-PS-ZnO nanocomposites were prepared by the simple solution mixing method. The anticorrosive properties of nanocomposite coatings were investigated on iron coupons and compared to that of pure PANI, PANI-ZnO nanocomposite, PANI-PS composite. The effect of a filler percent (ZnO) on the anticorrosive performance of PANI-PS-ZnO nanocom-posite was studied. PANI-PS-ZnO nanoco-mposite with an optimal percentage of ZnO was characterized with TGA, FT-IR and SEM techniques.

2. EXPERIMENTAL

2.1. Chemicals

Aniline, ammonium persulfate (APS), tetrahydrofurane (THF), sodium chloride (NaCl), hydrochloric acid (HCl) 37%, were all purchased from Merck Company. Aniline monomer was distilled two times before use. ZnO nanoparticles with the average particle size of 60 nm (purity 99.9%) were used.

Polystyrene (GPPS grade) was purchased from Petrochemical Company of Tabriz.

2.2. Preparation of PANI-PS-ZnO Nanocomposite

3g aniline was dissolved in 25 ml of HCl (0.5 M) and 1.5g ZnO nanoparticles were added to aniline solution. 7.5g APS as an initiator was dissolved in 25ml HCl (0.5 M) and was dropwisely added to aniline solution in 0 ºC, under vigorous stirring. The appearance of green color indicates the formation of PANI.

After the end of initiator addition, the mixture was stirred for 2 h in 0 ºC, to complete the reaction of polymerization. Finally, prepared PANI-ZnO nanocompo-site was filtered and washed with distilled water to remove oligomers and residuals, and was dried in 50˚C.

To prepare PANI-PS-ZnO nanocomposite with 3 different weight percentages of ZnO nanoparticles, 0.5 g PS was dissolved in 40 ml THF. Then, 0.025g PANI-ZnO nanocomposite was added to PS solution and stirred for 2h. PANI-PS-ZnO nanocomposite with 10 and 15 weight percentages of ZnO nanoparticles were

prepared by adding of 0.05 and 0.075g of PANI-ZnO nanocomposite, respectively. Pure PANI was prepared in the absence of ZnO nanoparticles.

2.3. Working Electrode Preparation

Iron coupons (1 cm ×1 cm × 0.1cm) were used as working electrode. Polyester lacquer was used to mount the behind and edges of the iron samples. Before corrosion tests, iron surfaces (with the surface area of 1 cm^2) were polished using 200 to 800 grade emery papers and washed using distilled water and acetone to remove any contaminations.

The surfaces of iron coupons were coated by a thin layer (40 µm) of PANI-PS-ZnO nanocomposites by solution casting method. The solvent (THF) evaporation was performed in environment temperature for 24 h.

Coatings of PANI, PANI-ZnO nanocomposite and PANI-PS composite were prepared with similar thickness, for comparison of their anticorrosive properties with PANI-PS-ZnO nanocomposites.

2.4. Corrosion Tests

Electrochemical corrosion test methods were selected to study the anticorrosive performance of pure, composite or nanocomposite coatings.

A conventional three electrode electrochemical cell was used to record Tafel plots. Iron sample with or without coating, Pt and SCE were used as working, counter and reference electrode, respectively. Iron coupon without coating was used as **a** reference sample. In the absence of counter electrode, a two electrode electrochemical cell system was used for open circuit potential (OCP) measurements.

Sodium chloride solution (3.5%) was used as an electrolyte in corrosion tests. Before corrosion test, all samples were immersed in sodium chloride solution (3.5%) for 80 min to reach equilibrium.

2.5. Characterization

A galvanostat/potentiostat (Autolab/PGSTAT302N) and three-electrode electrochemical cell system included of an iron sample (coated with composite, nanocomposite or pure polyaniline) as working electrode, a platinum gauze as counter electrode and an SCE as reference electrode were used for corrosion tests.

Bruker, Tensor 27 spectrophotometer was used to record the Fourier transform infrared (FT-IR) spectra of ZnO nanoparticles, pure PANI, PS and PS-[PANI-ZnO 10%] nanocomposite.

The surface morphology of PS-[PANI-ZnO 10%] nanocomposite was studied by scanning electron microscopy (SEM) of Vegall-Tescan Company and thermogravimetry (TGA) for ZnO nanoparticles, pure PANI, PS and PS-[PANI-ZnO 10%] nanocomposite were obtained by PL-TGA (Polymer Laboratories).

Cyclic voltammetry (CV) studies were performed with a conventional three-electrode electrochemical cell by using gold film coated by PS-[PANI-ZnO 10%] nanocomposite as working electrode (area=0.25 cm^2) in combination with platinum counter and Ag/AgCl reference electrodes.

3. RESULTS AND DISSCUTION

3.1. OCP measurements

Open circuit potential OCP measurements of PANI, PANI-ZnO, PANI-PS, PS-[PANI- ZnO 5%], PS-[PANI- ZnO 10%] and PS-[PANI- ZnO 15%] coated iron samples were carried out versus to time in NaCl (3.5%) electrolyte. The OCP values of coated iron coupons versus to SCE reference electrode against to time are shown in Fig. 1.

According to the Fig. 1, the potential of the electrode as the corrosion potential of coated samples was decreased with the passing of time and reached to the final equilibrium values.

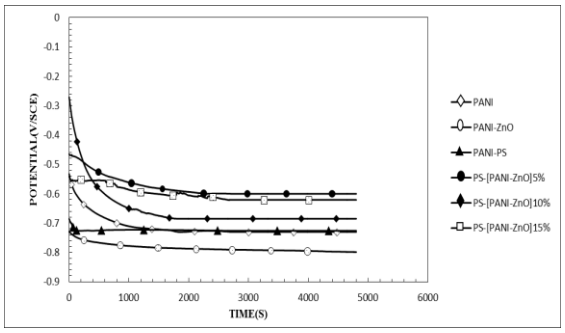

Figure 1. *OCP values of iron samples coated with PANI, PANI-ZnO, PANI-PS, PS-[PANI-ZnO 5%], PS-[PANI-ZnO 10%] and PS-[PANI-ZnO 15%] coatings in NaCl (3.5%) solution.*

The comparison of equilibrium OCP values of iron coupons shows that the final equilibrium OCP values of iron coupons, coated with PANI and PANI-PS coatings, are similar values.

The addition of ZnO nanoparticles to PANI coating causes to decrease in the final OCP values of PANI-ZnO coating by improving the cathodic protection of coating. Also, in PANI-PS-ZnO nanocomposite coatings, the barrier properties of coatings can improve with the addition of PS and the cathodic protection of coating can improve with the addition of ZnO.

Fig. 1 shows that the equilibrium OCP values of PANI-PS-ZnO nanocomposite coated samples are higher than that of PANI, PANI-PS and PANI-ZnO composite coated samples.

3.2. Tafel plots

Tafel plots were recorded in NaCl electrolyte (3.5%) by potential scanning from equilibrium toward positive and negative potentials against SCE reference electrode (Fig. 2). The anticorrosion performance of pure PANI, PANI-PS, PANI-ZnO, PS-[PANI-ZnO 5%], PS-[PANI-ZnO 10%] and PS-[PANI-ZnO 15%] coatings on iron coupons was evaluated by analyzing of slops of Tafel plots.

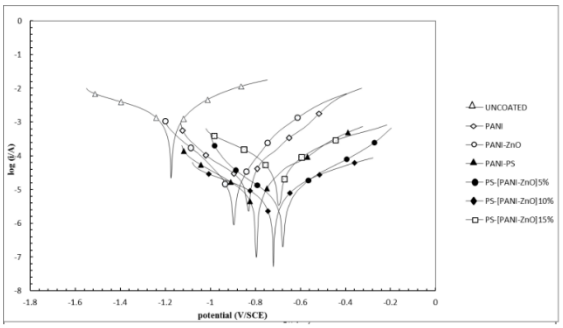

Figure 2. *Tofel plots of iron sample: (△) uncoated, coated with: (◇) PANI, (○) PANI-ZnO, (▲) PANI-PS, (●) PS-[PANI-ZnO 5%], (◆) PS-[PANI-ZnO 10%] and (□) PS-[PANI-ZnO 15%] coatings in NaCl (3.5%) solution.*

The values of corrosion potential, corrosion current and corrosion rate obtained from Tafel slope analysis of uncoated and coated iron samples have been shown in Table 1.

Table1. *Corrosion current and corrosion potential values of iron samples uncoated and coated with PANI, PANI-ZnO, PANI-PS, PS-[PANI-ZnO 5%], PS-[PANI-ZnO 10%] and PS-[PANI-ZnO 15%] coatings in NaCl (3.5%) solution.*

Coatings	Corrosion rate (mm/year)	E_{corr} (mV/SCE)	i_{corr} (µA)
Uncoated	7.3	1174-	631
PANI	0.46	-832	40
PANI-ZnO	0.29	-894	25
PANI-PS	0.10	-795	8.9
PS-[PANI-ZnO 5%]	0.073	-676	6.3
PS-[PANI-ZnO 10%]	0.046	-720	4
PS-[PANI-ZnO 15%]	0.45	-694	39

The values of corrosion rate (mm/year) can be calculated as follows [22]:

$$corrosion\ rate = k_1 \frac{i_{cor}}{\rho} EW \qquad (1)$$

k_1 = 0.0032,
i_{cor}= corrosion current (μA)
ρ =7.87 g/cm^3 for iron, and
EW is the equivalent weight of element =28 for iron.

According to Fig. 2 and Table 1, by coating PANI on iron sample the corrosion current value is decreased. The addition of the ZnO nanoparticles and PS polymer chains in PANI coating cause a further decrease in the corrosion current of iron sample. The maximum decreasing of the corrosion current of iron sample is obtained by PS-[PANI-ZnO 10%]. In this case, corrosion current of PS-[PANI-ZnO 10%] coating is about 160 and 15 times lower than that of uncoated and pure PANI coated iron samples respectively.

Superior anticorrosive property of PANI-PS-ZnO coatings (especially PS-[PANI-ZnO 10%]) are because of using the protection properties of three different components, including PS as barrier coating, ZnO as n-type semiconductor and PANI as p-type semiconductor.

Electroactivity

The film cast from PS-[PANI-ZnO 10%] nanocomposite was used for cyclic voltammetry studies. Fig. 3 shows the cyclic voltammograms of PS-[PANI-ZnO 10%] nanocomposite film in HCl (1M) as the electrolyte for 1st and 20th scans at 50 mV/s scan rate. The results showed that, the prepared film present two separate oxidation and reduction responses that indicate the PS-[PANI-ZnO 10%] nanocomposite is electroactive, similar to pure PANI. In addition, comparison of 1st and 20th scans showed that the electroactivity property of nanocomposite is reversible and stable.

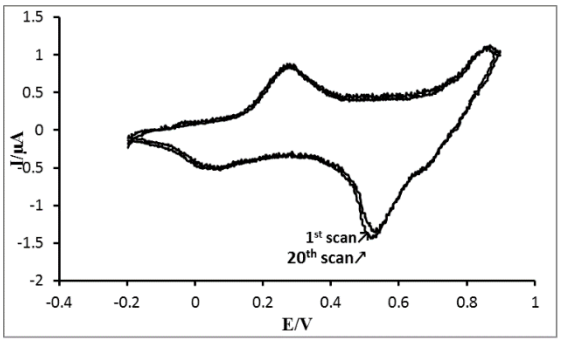

Figure 3. *1st and 20th Cyclic voltammograms of PS-[PANI-ZnO 10%] nanocomposite in 0.5 M HCl, scan rate of 50 mV/S, electrode area 0.25 cm^2*

3.3. FT-IR spectrum

In the FT-IR spectrum of pure PANI in curve [a] of Fig. 4 the absorption peaks at 140 cm^{-1} and 1580 cm^{-1} are attributed to the C-C stretching mode of benzonoid and quinoid rings in PANI chains respectively. The peaks at the wavenumbers of 1290 cm^{-1} and 3600 cm^{-1} are assigned to the C-N and N-H stretching bonds of the secondary amine group, respectively [7].

FT-IR spectra of ZnO (curve [b] of Fig. 4) shows three significant absorption peaks at the wavenumbers of 3500, 1500 and 400-600 cm^{-1}. The absorption band at 400-600 cm^{-1} belongs to Zn-O stretching vibration. The peak near 1500 cm^{-1} is attributed to H-O-H bending vibration mode due to the presence of moisture [7].

The IR spectrum of PS (curve [c] of Fig. 4) showed absorption bands at 3050 and 2850 cm^{-1} that can be assigned to aromatic and aliphatic C-H stretchings, respectively. The peaks at 1600 and 1500 cm^{-1} are attributed to aromatic C=C stretchings. The C-H deformation vibration band of benzene ring hydrogen's appeared at 950 cm^{-1}[17].

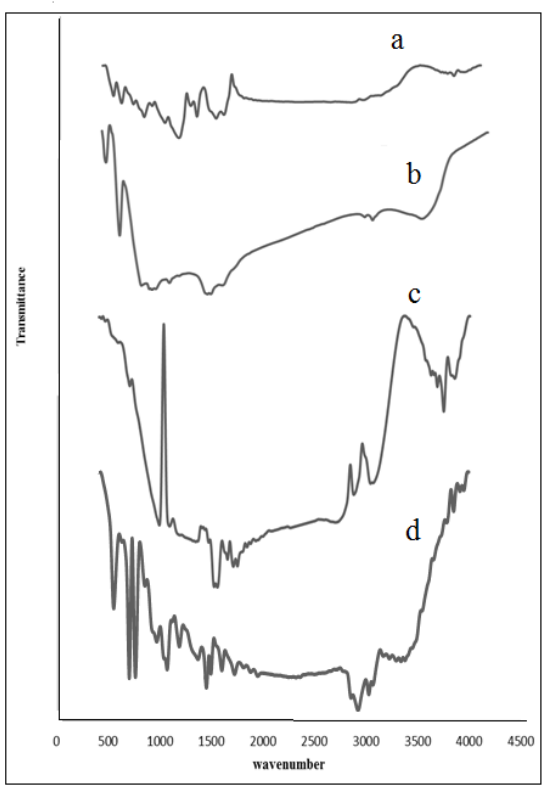

Figure 4. *FT-IR spectrum of [a] PANI, [b] ZnO, [c] PS, [d] PS-[PANI-ZnO 10%] nanocomposite.*

Curve [d] in Fig. 4 shows the FT-IR spectrum of PS-[PANI-ZnO 10%] nanocomposite. This curve exhibits bands characteristic of polyaniline, PS and ZnO which confirm the presence of three components in the PS-[PANI-ZnO 10%] nanocomposite. The absorption band near 500 cm^{-1} is the characteristic peak of Zn-O nanoparticles (stretching vibration).The peaks related to the aromatic C-H stretching vibration of PS near 3000 cm^{-1}. Curve [d] in Fig. 4 shows the peaks related to the quinoid rings and C-C stretching mode of benzonoid respectively at wave numbers of 1560 cm^{-1} and 1480 cm^{-1}, and the C-N stretching mode of PANI at 1270 cm^{-1}. The shift of all peaks related to the PANI in PS-[PANI-ZnO 10%] nanocomposite (curve d of Fig. 4) to lower wave numbers compared to that of pure PANI (curve [a] of Fig. 4), confirms the presence of some interactions between PANI, PS and ZnO nanoparticles [7].

3.4. SEM micrographs

The morphology of PS-[PANI-ZnO 10%] nanocomposite coating was studied by scanning electron microscopy (SEM) technique. Two SEM micrographs of PS-[PANI-ZnO 10%] nanocomposite coating has been shown in Fig. 5. According to these images blending of three components of nanocomposite was uniformly carried out and ZnO nanoparticles with diameter sizes of about 60 nanometers have been distributed in the polymer matrix.

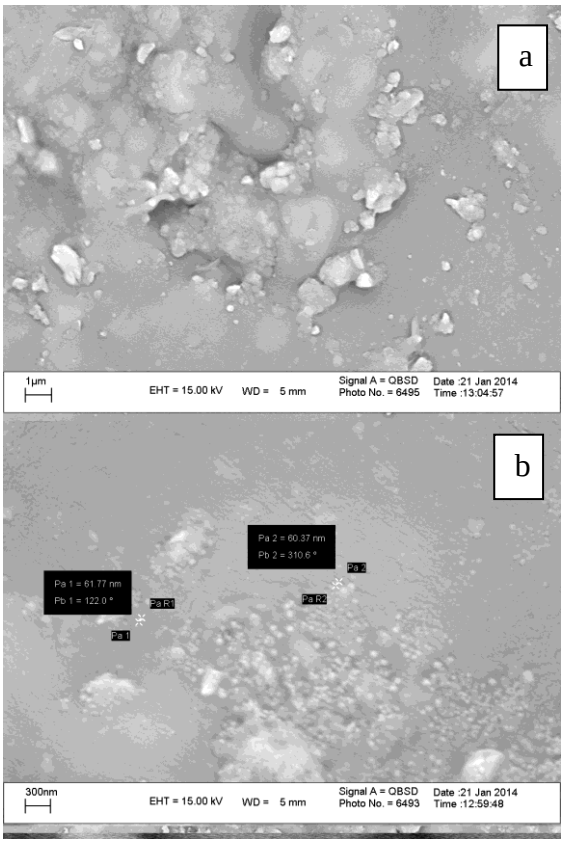

Figure 5. *SEM micrographs of PS-[PANI-ZnO 10%] nanocomposite, [a] 1 µm and [b] 300 nm.*

3.5. Thermogravimetry Analysis

The thermogravimetric analysis (TGA) of ZnO nanoparticles, pure PANI, PS and PS-[PANI-ZnO 10%] under heating rate of 10 °$Cmin^{-1}$ have been shown in Fig. 6. The results show that ZnO nanoparticles are very stable and weight loss is not observed in the temperature range of 50-800 °C. It can be seen that in the TGA curve of PS, weight loss occurring at 450 °C is due to the degradation of PS and it is completed

in 500°C. The results indicate that the initial mass loss of PANI at temperature ranges of 200-300 °C is due to release of water and removal of solvent or dopant anions. Also, the weight loss occurring around 400 °C is due to the decomposition of the PANI chains. The results indicate that the trend of [PS/PANI-ZnO 10%] nanocomposite degradation is similar to PANI and PS.

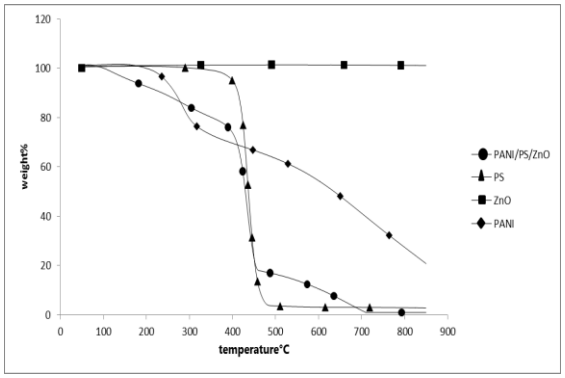

Figure 6. *TGA results of (◆) PANI, (▲) PS, (■) ZnO, (●) PS-[PANI-ZnO 5%].*

However, in PS-[PANI-ZnO 10%] nanocomposite, decomposition is improved in comparison to PANI at temperature ranges of about 300-400 °C and to PS at temperature ranges of about 450- 650 °C. It is probably due to the presence of a strong interaction at the interface of ZnO and PANI [23].

4. CONCLUSION

In the present work, PANI-ZnO nanocomposite was successfully synthesized by chemical polymerization of aniline in the presence of ZnO nanoparticles. 5, 10 and 15 percentages of PANI–ZnO nanocomposite were added to a solution of PS in THF to obtain PS-[PANI-ZnO 5%], PS-[PANI-ZnO 10%] and PS-[PANI-ZnO 15%] nanocomposites. The anticorrosive property of the prepared nanocomposites was studied by open circuit potential (OCP) and Tafel techniques in 3.5% NaCl solution as corrosive environment. It was demonstrated that the best corrosion protection effect belongs to the coating of PS-[PANI-ZnO 10%] nanocomposite in comparison to that of pure PANI, PANI–ZnO nanocomposite, PANI-PS composite and two other PANI-PS-ZnO nanocomposite coatings. The electroactivity of PS-[PANI-ZnO 10%] nanocomposite was studied and confirmed by CV studies. To characterize the composition and structure of PS-[PANI-ZnO 10%] nanocomposite, FTIR spectroscopy and SEM techniques were used. Also, to study of thermal stability of PS-[PANI-ZnO 10%] nanocomposite, TGA was used.

REFERENCES

1. Mirmohseni A., Oladegaragoze A., Farbodi M. (2008). "Synthesis and Characterization of Processable Conducting Polyaniline/Polystyrene Composite," *Iranian Polymer Journal,* 17: 135-140.
2. Zhou W., Yu Y., Chen H., DiSalvo F. J., Abruna H. D. (2013). "Yolk–Shell Structure of Polyaniline-Coated Sulfur for Lithium–Sulfur Batteries," *J. Am. Chem. Soc.* 135: 16736–16743.
3. Kunzo P., Lobotka P., Kovacova E., Chrissopoulou K., Papoutsakis L., Anastasiadis S. H., Krizanova Z., Vavra I. (2013). "Nanocomposites of polyaniline and titania nanoparticles for gas sensors," *physica status solidi (a),* 210: 2341–2347.
4. Nabid M. R., Sedgh R., Sharifi R., Abdi Oskooie H., Heravi M.M., (2013). "Removal of toxic nitrate ions from drinking water using conducting polymer/MWCNTs nanocomposites," *Iranian Polymer Journal*, 22(2): 85-92.
5. Araujo J. R., Adamo C. B., Costa Silva M. V., De Paoli, M. A. (2013). "Antistatic-reinforced biocomposites of polyamide-6 and polyaniline-coated curauá fibers prepared on a pilot plant scale," *Polymer Composites*, 34: 1081–1090.
6. Faisal M., Khasim S. (2013). "Polyaniline–antimony oxide composites for effective broadband EMI shielding," *Iranian Polymer Journal*, 22: 473-480.
7. Olad A., Nosrati R. (2013). "Preparation and corrosion resistance of nanostructured PVC/ZnO–polyaniline hybrid coating," *Progress in Organic Coatings*, 76: 113– 118.

8. Olad A., Naseri B. (2010). "Preparation, characterization and anticorrosive properties of a novelpolyaniline/clinoptilolite nanocomposite," *Progress in Organic Coatings*, 67: 233–238.
9. Mahulikar P. P., Jadhav R. S., Hundiwale, D. G. (2011). "Performance of Polyaniline/TiO2 Nanocomposites in Epoxy for Corrosion Resistant Coatings," *Iranian Polymer Journal*, 20: 367-376.
10. Olad A., Barati M. Shirmohammadi H. (2011). "Conductivity and anticorrosion performance of polyaniline/zinc composites:Investigation of zinc particle size and distribution effect," *Progress in Organic Coatings*, 72: 599– 604.
11. Zhu H., Hou J., Qiu R., Zhao J., Xu J. (2014). "Perfluorinated lubricant/ polypyrrole composite material: Preparation and corrosion inhibition application," *Journal of Applied Polymer Science*. 131:40184.
12. Liang C., Chen W., Huang N. (2013). "Preparation and Corrosion Resistance of Polythiophene Film/Square Wave Oxide Layer of Stainless Steel. *Journal of Materials Engineering*, 3: 73-78.
13. Afzal A. B., Akhtar M. J., Ahmad M. (2010). "A Morphological studies of DBSA-doped polyaniline/PVC blends," *Journal of Electron Microscopy*, 59: 339.
14. Kondawar S. B., Anwane S. W., Nandanwar D. V., Dhakate S. R. (2013). "Carbon nanotubes reinforced conducting polyaniline and its derivative poly(*o*-anisidine) composites," *Adv. Mat. Lett*. 4: 35-38.
15. Baldissera A. F., Souza J. F., Ferreira C. A. (2013). "Synthesis of polyaniline/clay conducting nanocomposites," *Synthetic Metals*, 183: 69– 72.
16. Ashis D., Sukanta D., Amitabha D. (2004). "Characterization and dielectric properties of polyaniline–TiO_2 nanocomposites," *Nanotechnology*, 15: 1277.
17. Kaniappan K., Latha S. (2011). "Certain Investigations on the Formulation and Characterization of Polystyrene /Poly(methyl methacrylate) Blends," *International Journal of ChemTech Research*, 3: 708-717.
18. Afzal A. B., Akhtar M.J. (2012). "Effects of silver nanoparticles on thermal properties of DBSA-doped polyaniline/PVC blends," *Iranian Polymer Journal*, 21:489-496.
19. Mohammad A., Rostami A. (2016). "Effect of Concentration of Surfactant and Additive on Morphology of Polyaniline Nanocomposites Prepared in Aqueous Solution," *International Journal of Nanoscience and Nanotechnology*, 12: 37-43.
20. Olad A., Khatamian M., Naseri B. (2010). "Preparation of Polyaniline Nanocomposite with Natural Clinoptilolite and Investigation of Its Special Properties," *International Journal of Nanoscience and anotechnology*, 6: 43-52.
21. Sathiyanarayanan S., Jeyaram R., Muthukrishnan S., Venkatachari G. (2009). "Corrosion Protection Mechanism of Polyaniline Blended Organic Coating on Steel" *Journal of the Electrochemical Society*, 156: 127-134.
22. Abdelhamid Taha N., Morsy M. (2015). "Study of the behavior of corroded steel bar and convenient method of repairing" *HBRC Journal*, in press.
23. Mostafaei A., Zolriasatein A. (2012). "Synthesis andcharacterization of conducting polyaniline nanocomposites containing ZnO nanorods," *Progress in Natural Science.Materials International*, 22: 273–280.